Disease specific alterations in the olfactory mucosa of patients with Alzheimer's disease

Riikka Lampinen[1*], Mohammad Feroze Fazaludeen[1*], Simone Avesani[2], Tiit Örd[1], Elina Penttilä[3], Juha-Matti Lehtola[4,5], Toni Saari[4], Sanna Hannonen[4,5], Liudmila Saveleva[1], Emma Kaartinen[1], Francisco Fernandes Acosta[1], Marcela Cruz-Haces[1], Heikki Löppönen[3], Alan Mackay-Sim[6], Tarja Malm[1], Minna Kaikkonen-Määttä[1], Anne M Koivisto[4,5,7,8], Anthony R White[9], Rosalba Giugno[2], Sweelin Chew[1], Katja M Kanninen[1]

*Equal contribution

[1] University of Eastern Finland, A. I. Virtanen Institute, Kuopio, Finland

[2] University of Verona, Department of Computer Science, Verona, Italy

[3] University of Eastern Finland and Kuopio University Hospital, Department of Otorhinolaryngology, Kuopio, Finland

[4] University of Eastern Finland, Brain Research Unit, Department of Neurology, Kuopio, Finland

[5] Kuopio University Hospital, Department of Neurology, Kuopio, Finland

[6] Griffith University, Griffith Institute for Drug Discovery, Brisbane, Australia

[7] University of Helsinki, Department of Neurosciences, Helsinki, Finland

[8] University Hospital of Helsinki, Department of Geriatrics, Helsinki, Finland

[9] QIMR Berghofer, Medical Research Institute, Department of Cell and Molecular Biology, Mental Health Program, Brisbane, Australia

ABSTRACT

Olfactory dysfunction manifests in early stages of neurodegeneration in several disorders of the central nervous system. The sense of smell is orchestrated by the cells of the olfactory mucosa located in the upper nasal cavity, however, it is unclear how this tissue reflects key neurodegenerative features in Alzheimer's disease (AD). Here we report that olfactory mucosa (OM) cells of patients with AD secrete increased amounts of toxic amyloid-beta. We detail cell-type specific gene expression patterns, unveiling 154 differentially expressed AD-associated genes compared to the cognitively normal controls, and 5 distinct cell populations in the cultures, together with disease-associated subpopulations. Overall, coordinated alteration of RNA and protein metabolism, inflammatory processes and signal transduction were observed in multiple cell types, suggesting a key role in AD pathophysiology. Our results demonstrate the potential of OM cultures as a new cellular model for AD. Moreover, for the first time we provide single cell transcript data for investigating the molecular and cellular mechanisms of AD in the OM.

INTRODUCTION

The olfactory mucosa (OM) is critical for the sense of smell and in direct contact with the brain [1]. Anosmia, loss of the sense of smell, has been linked to the early phases of several neurodegenerative diseases including Alzheimer's disease (AD) [1,2]. AD pathology is typified by extracellular beta-amyloid (Aβ) plaques, intracellular neurofibrillary tangles consisting of hyperphosphorylated tau protein, cell loss, neuroinflammation, and metabolic stress. Young-onset or familial AD is rare and caused by mutations in genes encoding the y-secretase complex members presenilin 1 (PS1) or presenilin 2 (PS2), and in the amyloid precursor protein (APP). However, late-onset AD (LOAD) is the most common disease form and the major risk gene for

this is *APOE*, the ε4 allele of which confers a 12-fold increase in disease risk in homozygous carriers [3]

Nasal secretions of LOAD patients contain elevated amounts of Aβ and phosphorylated tau [4–6]. *Post mortem* histological analysis of AD OM have revealed increased Aβ aggregation in the apical surface of the epithelium and intracellular Aβ has been detected in anosmic LOAD patients [7]. In addition, immunostaining for filamentous tau has been observed inside neurites and in neuronal soma, resembling intracellular neurofibrillary tangles, in cells close to the OM basal membrane [8]. However, little information exists on cell-type specific, AD-related alterations to olfactory mucosal cells. The only cell-type specific observations thus far are from olfactory neurons in *post mortem* analyses of AD patients [9,10], and from OM-derived neuroblast cultures that exhibited elevated oxidative stress and altered APP processing [11,12]. Therefore, the OM and especially the olfactory receptor neurons have been reported to show AD-linked pathological changes. The cellular content of the biopsied OM of healthy individuals was recently assessed by single-cell RNA sequencing (scRNA-seq) [13], but cell-type specific alterations occurring in AD OM remain unknown. Human OM cells can be obtained for *in vitro* studies with a relatively non-invasive biopsy, thus providing a way of gaining access to neural tissue of living individuals [13,14].

In this study, we harvested OM biopsies from age-matched cognitively healthy individuals and patients with LOAD to profile AD-linked functional alterations and changes in gene expression at the single-cell level. We observed significantly increased secretion of pathological Aβ from the cultured AD OM cells and 154 differentially expressed genes (DEGs) associated with AD including cell-type specific DEGs. Furthermore, these DEGs enrich for pathways including RNA and protein metabolism, inflammatory processes and signal transduction. Together, these results

support the utility of the OM as a physiological *in vitro* model of AD and provide a unique cellular-level view of transcriptional alterations associated with AD pathology.

RESULTS

Secretion of $A\beta_{1-42}$ is increased in AD OM cells

To test whether OM cells from AD donors exhibit the typical pathological hallmarks of the disease, we first analyzed intracellular and secreted levels of $A\beta_{1-42}$, $A\beta_{1-40}$, total tau, and tau phosphorylated at threonine 181 *(P_{181}-tau)* in cognitively healthy individuals and patients with AD using ELISA (Fig. 1). A significant increase of secreted $A\beta_{1-42}$ was observed in AD OM cells (18.52 ± 7.590 pg/mg protein, p= 0.0366) when compared to cells derived from cognitively healthy individuals. In addition, the ratio of secreted $A\beta_{1-42}$ over $A\beta_{1-40}$ was higher in AD OM cells, in comparison to controls (0.2230 ± 0.06919, p=0.0096). No difference was observed in levels of $A\beta_{1-40}$, total tau, or P_{181}-tau. Likewise, these proteins remained unaltered in the plasma of patients with AD. While the levels of secreted $A\beta_{1-42}$ were not found to correlate to the status of the donor's sense of smell, all experimental groups did not have both anosmic and hyposmic individuals in them (Supplementary figure 1a). However, the OM cells of the AD patients with hyposmia secreted notably increased amounts of $A\beta_{1-42}$ (30.42 ± 13.34 pg/mg protein, p = 0.0847) in comparison to the cognitively healthy individuals with hyposmia. Furthermore, there was no significant difference in the secretion $A\beta_{1-42}$ from OM cells obtained from donors with at least one APOE ε4 allele compared to donors with two APOE ε3 alleles (Supplementary figure 1b).

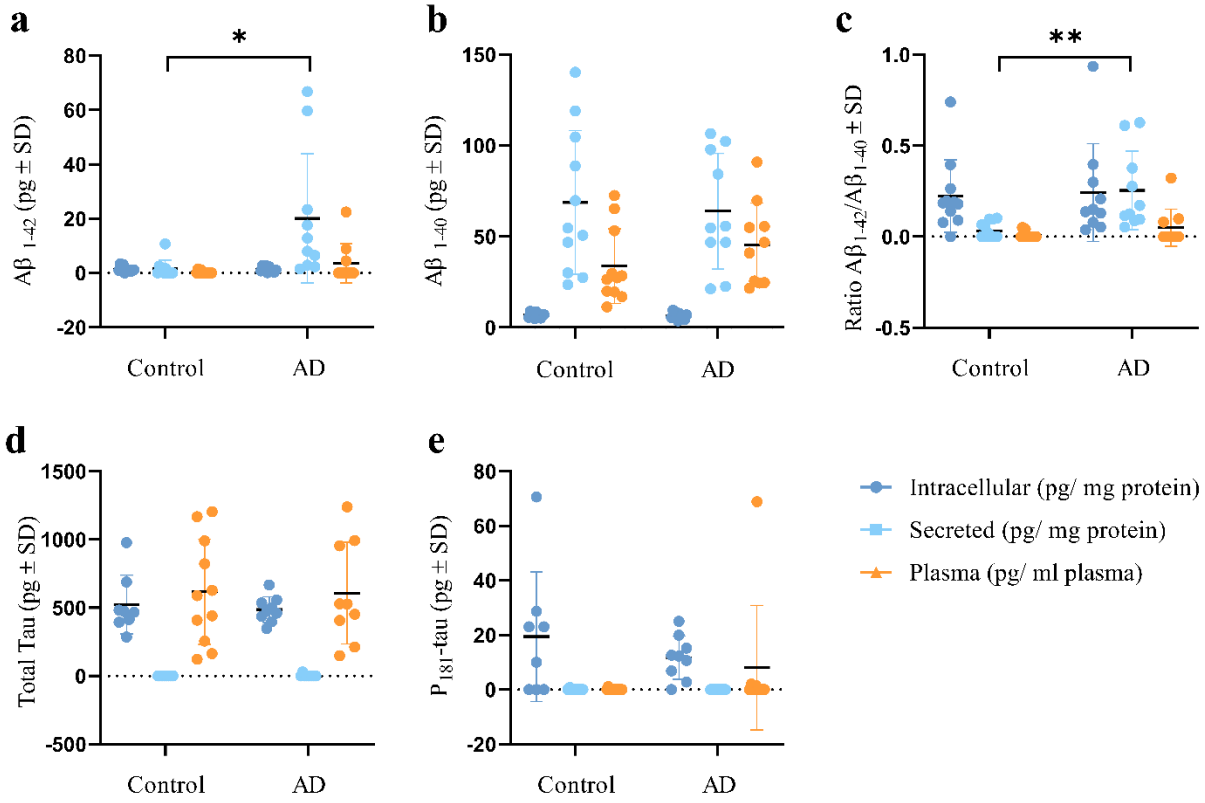

Figure 1. Aβ secretion is increased in AD OM cells. *OM cells harvested from biopsies were plated cultured for 7 days prior to collection of culture media and cell lysates for ELISA assays. The results were normalized to the total amount of protein measured from cell lysates.* ***a)*** *ELISA assay for $A\beta_{1\text{-}42}$.* ***b)*** *ELISA assay for $A\beta_{1\text{-}40}$.* ***c)*** *Ratio of $A\beta_{1\text{-}42}$ over $A\beta_{1\text{-}40}$. In Aβ ELISA assays N=11 for cognitively healthy controls and N=10 for AD patients.* ***d)*** *ELISA assay for total tau.* ***e)*** *ELISA assay for P_{181}-tau. In tau ELISA assays N=8 for cognitively healthy controls and N=9 for AD patients. Quantification of secreted and intracellular $A\beta_{1\text{-}42}$, $A\beta_{1\text{-}40}$, tau and P_{181}-tau between control and AD OM cells were performed with t test (unpaired, Welch's correction).* ***a*** ** $p < 0.05$.* ***c*** *** $p < 0.01$. For all graphs data is presented as mean ± SD and calculated the statistics as difference in means ± SEM.*

Cytokine secretion is not altered in AD OM cells

To profile the innate immunity of OM cells, we next used the CBA array to analyze the levels of 5 cytokines in OM cells and plasma of cognitively healthy control subjects and AD patients. Secreted or intracellular cytokine levels of AD OM cells were not altered in comparison to OM cells from cognitively healthy subjects (Figure 2). However, the plasma samples of AD patients contained significantly increased amounts of tumor necrosis factor (TNF) compared to plasma collected from cognitively normal individuals (1.324 ± 0.2277 pg/ml plasma, $p < 0.0001$) (Fig. 2f).

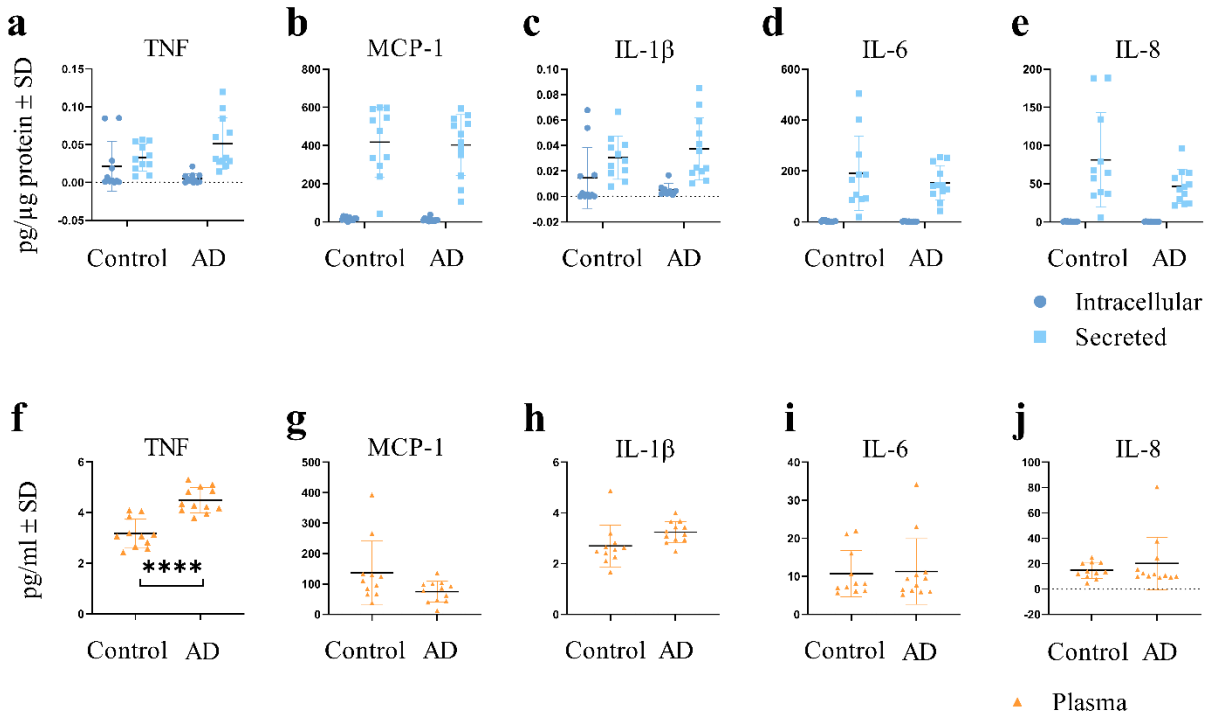

Figure 2. Cytokine levels are unaltered in AD OM cells. *OM cells harvested from biopsies were plated and cultured for 7 days prior to collection of culture media and cell lysates for the CBA array. The results were normalized to the total amount of protein measured from cell lysates.* ***a-e)*** *Levels of intracellular and secreted cytokines in OM cells. N = 11 for cognitively healthy controls*

and N = 12 for AD patients. ***f-j)*** *Levels of cytokines in plasma samples. N = 11 for cognitively healthy controls and N = 12 for AD patients. Quantification of secreted, intracellular or plasma cytokines between control and AD cells was performed with t test (unpaired, Welch's correction). **** $p < 0.0001$. For all graphs data is presented as mean ± SD and calculated the statistics as difference in means ± SEM. TNF: tumor necrosis factor, MCP-1: monocyte chemoattractant protein 1, IL: interleukin.*

Cellular diversity of the human OM in health and AD

To investigate the cell type diversity and AD-associated cellular changes in the OM, we performed single-cell RNA sequencing (scRNAseq) of OM cultures derived from cognitively healthy controls and patients with AD (Fig. 3a). To reduce variability and exclude the possible effect of *APOE* ε4 allele on the observed results, OM cell lines from female donors with an *APOE* ε3/3 genotype (age average 72.4) were used for scRNA-seq.

We sequenced 10,816 live cells for the control library and 12,582 live cells for the AD library. The median number of genes per cell in the control and AD libraries was 4,066 and 3,336 respectively. After quality-control filtering 8,559 cells for controls and 10,086 for AD were obtained (Fig. 3b-c, suppl fig 2). Single cell transcriptomes were clustered in uniform manifold approximation and projection (UMAP) to assess cellular heterogeneity with the Seurat clustering combined with EnrichR and HumanBase tools. In the UMAP projection we found that libraries segregated well from one another. Six clusters were identified in the control library, consisting of neuronal progenitor cells, neuroepithelial cells, fibroblasts, smooth muscle cells, dendritic cells and chondrocytes (Fig. 3d). In the AD library the clusters were identified as neuronal progenitor cells,

neuroepithelial cells, fibroblasts, smooth muscle cells, dendritic cells and macrophages (Fig. 3e). Fig 3f shows the proportion of cell types present in the OM cultures of each donor. By proportion, the largest number of cells in the OM cultures were annotated as fibroblasts, neuroepithelial cells, and neuronal progenitor cells. The proportion of neuroepithelial cells was reduced in AD OM cultures (17.4% and 19.8% from total number of cells/ donor) compared to OM cells derived from cognitively healthy individuals (ranging from 26.5% to 29.4% from total number of cells/ donor). Notably, in AD OM cultures, cells annotated as epithelial cells covered almost one third of all the annotated cells (28.9% and 30.0% from total number of cells/ donor) and the proportion of smooth muscle cells was significantly reduced (2.7% and 1.5% from total number of cells/ donor) in comparison to OM cells of cognitively healthy individuals (ranging from 2.5% to 15.0% from total number of cells/ donor) (Fig. 3f). The analyses also revealed the presence of distinct cell populations when comparing cognitively healthy controls and AD patients. Macrophages and epithelial cells were only present in AD samples, whereas chondrocytes were found only in two of the three cognitively healthy donors (Fig. 3b, d and f). These cell type categories were used to characterize AD-related gene expression perturbations occurring in the OM on the level of single cells.

Differential expression analysis reveals AD-related alterations of gene expression in the OM

The single cell transcriptomic analysis of OM cells revealed an overall total of 154 AD-associated genes differentially expressed between the OM cell libraries of cognitively healthy control individuals and patients with AD. A total of 95 of the AD-associated DEGs were up-regulated and 59 AD-associated DEGs were down-regulated in the AD OM cells. Figure 3g illustrates a subset

of the most differentially expressed AD-associated genes between the OM libraries. *STC1*, T*FPI2*, *MMP1*, *CBX3* and *PABPC1* were the top five up-regulated DEGs and *SFRP2*, *MGP*, *SFRP1*, *IGFBP2* and *HTRA1* formed the top five most down-regulated DEGs. Given the increased secretion of $A\beta_{1\text{-}42}$ from the AD OM cells, we next investigated whether genes linked to APP processing were differentially expressed in the AD OM cells. Gene list analysis of the 95 AD-associated genes up-regulated in the AD OM cells with PANTHER (Protein Analysis Through Evolutionary Relationships, [15,16]) revealed three genes (*PCSK7*, *MMP1*, *MMP14*) annotated to the Alzheimer's disease-presenilin pathway (PANTHER pathway P00004). In addition, *PCSK7* annotated to the Alzheimer's disease-amyloid secretase pathway (PANTHER pathway P00003).

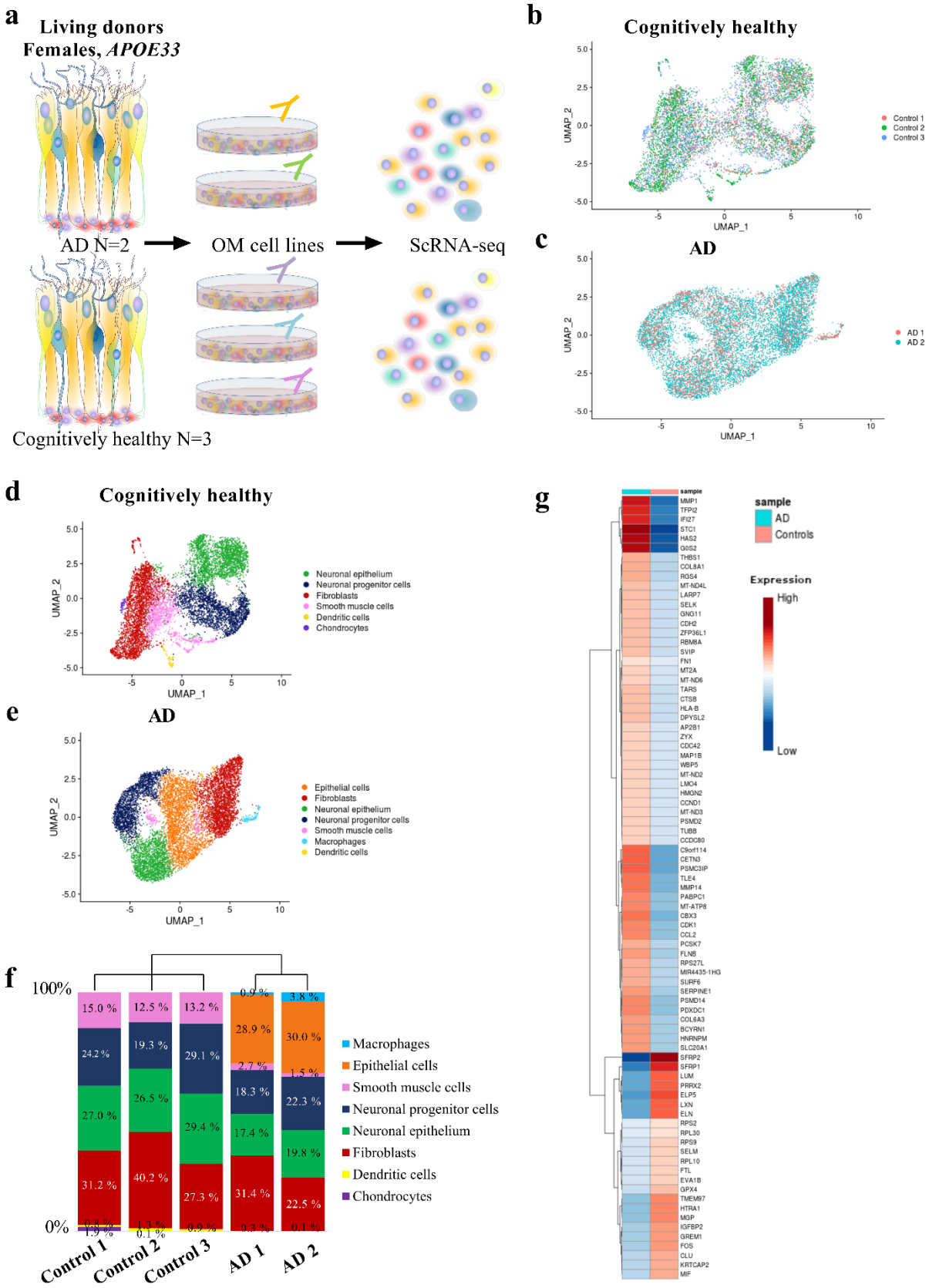

Figure 3. scRNA-seq data revealed AD-specific alterations in OM cells. a) *Schematic illustration of the sample material and scRNA-seq workflow.* ***b)*** *UMAP visualization of the clustering of single cells and showing by colors the cells derived from individual cognitively healthy donors.* ***c)*** *UMAP visualization of the clustering of single cells and showing by colors the cells derived from individual AD patients.* ***d)*** *Annotated cell types in samples in cognitively normal individuals, and* ***e)*** *in AD patients.* ***f)*** *Proportion (%) of cells derived from each donor per cell-type.* ***g)*** *Heatmap depicting a subset of the AD-related genes differentially expressed between AD and control libraries. The data is presented as the logarithm of the average expression in AD and control cells of the most differentially expressed genes (avg_logFC < -0.3, avg_logFC > 0.3).*

Analysis of individual cell types reveals distinctive AD-associated genes and pathways

In contrast to comparing overall transcriptomic changes between cognitively healthy donors and patients with AD, assessment of transcriptomic changes in individual cell-types revealed slightly altered numbers of AD-associated DEGs (Fig 4). Only 15 AD-associated DEGs were common to all five cell-types (Table 1). The up-regulated AD-associated genes, *PCSK7*, *MMP1* and *MMP14*, potentially linked to APP processing, were expressed by fibroblasts, neuroepithelial cells and neuronal progenitor cells (Fig 3g and Table 1). In addition, up-regulation of *MMP14* was detected in smooth muscle cells of AD patient OM. Collectively, these three genes are also associated with cytokine signaling in immune system and ECM organization. In AD, dendritic and neuroepithelial cells are most transcriptionally active with 164 and 112 up-regulated genes (Fig 4a, b). The most up- and down-regulated genes in each cell cluster were unique to the cell type (Fig 4c). Interestingly, dendritic cells exhibited the most unique, AD-associated DEGs (129 genes), which enrich for interferon and interleukin signaling (Fig 4b, d & suppl fig 3). Using the 154 DEGs

significantly up-regulated and down-regulated in AD shown in figure 3g, we performed Reactome pathway analysis and identified a total of 84 significantly enriched pathways. Enriched pathways were associated with RNA and protein metabolism (28), inflammatory processes (8), signal transduction (6), developmental biology (6) and neuronal system (3) (Fig 4d). Conversely, pathways enriched in control neuroepithelial cells and neuronal (or neural) progenitor cells include NMDA receptor activity (FLNB, TUBB4B, KNPA2) and SHH signaling (TUBA1B, PSDM14, PSMD2) (Fig 4d).

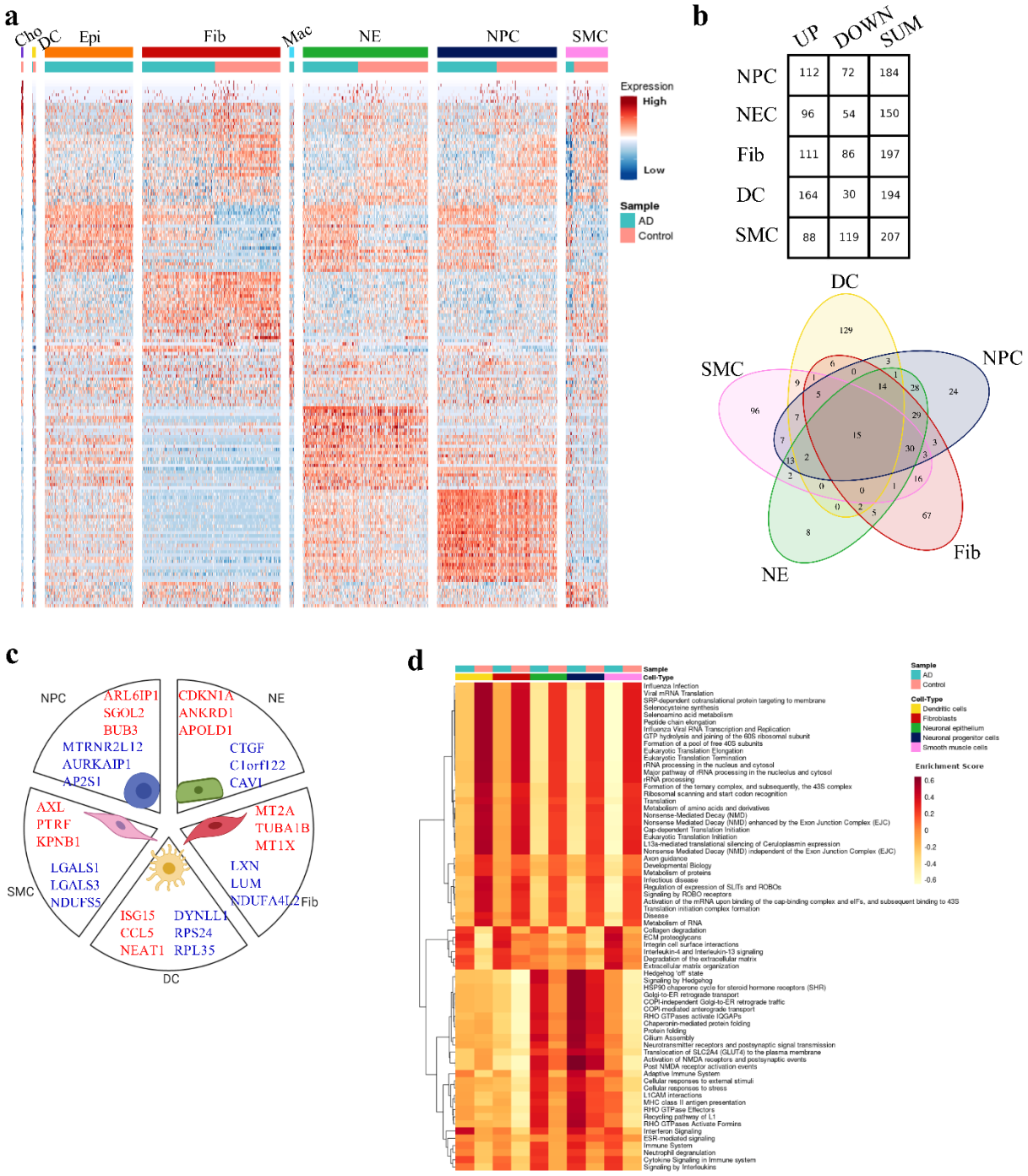

Figure 4. Cell type-specific pathways altered in AD a) *Heatmap depicting differential gene expression at the single-cell level for the most differentially expressed genes for each cell-type cluster separated by annotated OM cell-type clusters between donors with AD and cognitively*

healthy individuals. Each expression values are scaled and centered in 0. The range of expression values is from -4 to 4. ***b)*** *Numbers of differentially expressed AD-related genes by cell-types common for controls and AD shown as table and Venn-diagram.* ***c)*** *The top three up-regulated (in red) and down-regulated (in blue) AD-related and cell-type specific genes differentially expressed between control and AD OM by cell-type.* **d)** *Heatmap of the subset of differentially expressed pathways for cell-types common between AD and controls shows GSVA enrichment score of the pathways obtained for the DEGs with adjusted p-value <0.05. The enrichment score range is from -1 to 1. NPC, neuronal progenitor cells. NE, neuroepithelial cells. Fib, fibroblasts. DC, dendritic cells. SMC, smooth muscle cells. Cho, chondrocytes. Epi, epithelial cells. Mac, macrophages.*

DISCUSSION

Olfactory impairment is an early feature of AD, yet the human OM remains poorly studied to date. Although previous reports demonstrated by histological assessment the presence of pathology typical for the disease, cell-type specific changes in AD OM have not been studied. Here, we report the OM cell culture as a highly physiologically relevant model to study AD *in vitro*. Our results demonstrate the secretion of toxic Aβ by AD OM cells and the single-cell transcriptomic signature of these cells together with 154 differentially expressed and previously AD-associated genes involved in pathways namely related to RNA and protein metabolism, inflammatory processes and signal transduction.

The OM is composed of three primary components, the epithelium, basement membrane, and lamina propria. *In vivo*, the human OM consists of olfactory sensory neurons in various maturation stages, basal cells (stem cells), Bowman's gland cells, sustentacular cells, olfactory microvillar cells, olfactory ensheathing glial cells, vascular smooth muscle cells, blood cells, endothelial cells,

and immune cells as recently described [13]. We identified neuronal progenitor cells, neuroepithelial cells, dendritic cells, fibroblasts and smooth muscle cells as common cell types present in OM cell cultures of cognitively healthy controls and AD patients. Although some cell types remained unidentified, it is likely that the cultures do not contain all the cell types present in the OM *in vivo*. This could possibly be due to the more robust cell-types such as fibroblasts surviving the culture conditions better and dominating the more sensitive and low abundance sensory neurons. The presence of chondrocytes, found in two control donors, could be explained by a piece of cartilage remaining in the tissue during biopsy processing for OM cell cultures. While donor to donor variation in both groups was minimal with regards to the proportions of cell-types present, our analyses revealed the presence of epithelial cells and macrophages in the AD patient OM cultures, which were absent in the healthy donors. The presence of these cell populations in AD patients reflect disease-specific alterations to the OM, which may be in part explained by increased inflammation known to be a central pathological hallmark of the disease. However, studies with larger patient numbers are needed to confirm this finding.

Our findings reveal that OM cells can produce and secrete $A\beta_{1-40}$ and $A\beta_{1-42}$, with AD patient cells secreting significantly more $A\beta_{1-42}$ than cognitively healthy control cells. Prior literature demonstrates that the nasal mucosa or nasal secretions of AD patients also exhibit increased levels of Aβ [4,6–8,17]. Furthermore, the amount of $A\beta_{1-42}$ in the nasal area of transgenic Tg2576 mice modelling AD positively correlates with $A\beta_{1-42}$ deposition in their brain [18]. The fact that AD OM cells secrete increased levels of toxic Aβ demonstrates that this *in vitro* model shows the expected disease-specific pathological alterations. To deduce why $A\beta_{1-42}$ secretion is increased in AD OM cells, we found the expression of genes *PCSK7* and *MMP14* (logFC ranging from 0.31 to 0.40 and from 0.39 to 0.44, respectively) to be up-regulated in all the major cell types of the AD OM

cultures. Our pathway analysis of the 95 up-regulated genes in the AD OM cells revealed PCSK7, and MMP14 to be involved Alzheimer's disease-presenilin pathway (PANTHER pathway P00004, [16,17]). Both *PCSK7* and *MMP14* are linked to APP processing [19–21], although their role in APP processing in human OM has not been studied. PCSK7 is activated by metallothionein 3 (*MT3*), which in turn activates APP cleaving α-secretase and metalloprotease, ADAM10 [21].

In our data, we detect no changes in *MT3* expression. However, the gene expression levels of *MT2A* (metallothionein 2A) and its paralog gene *MT1X* (metallothionein 1X) were significantly up-regulated in AD OM derived fibroblasts (logFC 0.65 and 0.44, respectively). Previous studies have also demonstrated an increase in MT2A expression skin fibroblasts of AD patients [22]. Detailed studies into the effects of the heavy metal binding proteins on APP processing in OM would form an interesting future direction of research. Furthermore, as a possibly unique feature of APP processing in the human OM, we observed reduced expression of genes encoding for secreted frizzled related proteins (*SFRP1* logFC ranging between -0.89 and -0.59, and *SFRP2* logFC ranging between -1.62 and -0.65) in AD OM in all cell-types common between AD and control OM, excluding dendritic cells. In brains affected by AD, SFRP1 is known to be elevated and promote pro-amyloidogenic APP processing by negatively regulating the α-secretase ADAM10 activity [23]. Further experiments are needed to study the role of SFRPs on APP processing in the human OM.

Although hyperphosphorylated tau was detected in neurites in AD OM histological sections [8], we did not observe a change in levels of total or phosphorylated tau between AD and control OM cells. This lack of change is not surprising given that mature neurons were not detected in our OM cell cultures, where tau is expressed endogenously [24].

Multiple genome-wide association studies have found pathways related to metabolism and immune system to be altered in AD [25–27], thus supporting our findings of altered DEGs related to pathways including RNA and protein metabolism, inflammatory processes, signal transduction, developmental biology and neuronal system. We observed that immune system pathways were significantly enriched, which aligns with published studies [28,29]. Interestingly, neurotransmitter receptors and postsynaptic signal transmission, which are involved in intercellular communication and electrical signaling within the cell (for review see [30]), were enriched in neuronal epithelium, neuronal progenitors and smooth muscle cells. These results suggest an altered cell-cell communication in the AD OM.

We detected a small population of macrophages in AD OM cultures, which was absent in cognitively healthy control individuals. This may indicate resilient chronic inflammation, a renowned hallmark of AD [3]. Although our CBA results did not reflect AD OM cells to secrete more cytokines when compared to the controls, our pathway analysis revealed that AD-associated DEGs enrich for Cytokine Signaling, Interleukin-4, Interleukin-13 signaling pathways. We surmised that the small (< 4 %) population of macrophages would not contribute to overall changes in inflammatory signatures in AD OM cells. Longer culture periods or exposure to inflammatory stimuli may reveal differential cytokine profiles between the AD and control OM cultures, as previously demonstrated in healthy OM cells [31].

Beyond the OM, olfactory sensory cues are processed by the olfactory bulb, olfactory tract, piriform cortex, amygdala, entorhinal cortex, and hippocampus [32]. ScRNA-seq results by Grubman et al. on the AD entorhinal cortex and our findings have the following eight common DEGs between the control and AD groups [33]: *SERPINE1*, *IFI27*, *MT-ND2*, *MT-ND3*, *MAP1B*, *BCYRN1*, *ANGPTL4* and *HES1*. The presence of the common DEGs highlights the importance of these genes

in AD independently of the tissue type assessed and suggests that the entorhinal cortex and OM, both vulnerable to early AD pathogenesis, display disease-specific alterations that may have potential for early targeting.

In contrast to the widely used induced pluripotent stem cells (iPSCs) which have proven useful for modelling primarily monogenic diseases, OM cells present high research potential in complex age-related diseases, such as LOAD. While several studies have produced evidence that iPSCs lines can acquire a variety of genetic and epigenetic aberrations during the reprogramming process [34], the OM cells retain epigenetic alterations obtained throughout life [34]. In addition, OM cells are accessible from living donors, thus enabling repeated assessment of the disease-associated features during disease progression.

To open new avenues of therapy and to overcome the failure of neuron-targeting therapies for AD, current research focus is diverted towards non-neuronal cells. Albeit, further studies are needed to confirm the pertinence of the OM cells as a highly translational human cell model for AD. Our results emphasize the underexplored potential of this cell model for research purposes. Furthermore, 3D cell culture may promote AD-related disease phenotypes in OM, as demonstrated in iPSC-derived co-cultures (for review see [35]). Taken together, the results shown here clearly highlight the potential of the OM cells to reveal specific molecular mechanisms and cellular processes for future cellular studies and therapeutic intervention for AD. Moreover, these cells are expected to be useful for diagnostic purposes when harvested from individuals at early disease stages.

METHODS

Ethical considerations

The study was performed with the approval of the Research Ethics Committee of the Northern Savo Hospital District (permit number 536/2017) and a written informed consent was collected from all the subjects and proxy consent from the family members of persons with mild AD dementia.

Patients and OM cell cultures

A total of 12 voluntary study patients with AD type mild (CDR 1) dementia were recruited via Brain Research Unit, Department of Neurology, University of Eastern Finland. AD diagnostic examinations had been carried out at Brain Research Unit or at the Department of Neurology, Kuopio University Hospital prior to study recruitment. All the patients with AD dementia fulfilled the NIA-AA clinical criteria of progressive AD and MRI imaging or FDG-PET study had showed degenerative process or, in CSF biomarker examination was found biomarker (beta-amyloid, tau and phos-tau) changes typical to AD [36]. Eleven cognitively healthy control subjects were recruited via Department of Otorhinolaryngology, Kuopio University Hospital, Finland from patients undergoing a dacryocystorhinostomy (DCR) surgery, or from the already existing registries of the Brain Research Unit of University of Eastern Finland. Cognition of all the study patients were evaluated utilizing the Consortium to Establish a Registry for Alzheimer's Disease (CERAD) neuropsychological battery [37,38]. The age of the patients with AD and cognitively healthy control subjects age average 68.3 years and 70.6 years, respectively. For AD group 50% of the study subjects were males and 50% females, whereas for control subjects 27.3% were males and 72.7% females. A venous blood sample was taken from all study participants for use in *APOE*-genotyping. Based on genotyping, 66.7% of the patients with AD and 36.4% of cognitively healthy control subjects had at least one *APOE* ε4 allele. Patients and cognitively healthy study

participants were tested for their sense of smell for 12 odors (Sniffin' Sticks, Heinrich Burghart GmbH, Wedel, Germany) and classified as normal, hyposmic, or anosmic.

A piece of the OM was collected as a biopsy from the nasal septum, close to the roof of the nasal cavity as previously described [14]. The biopsy was kept on ice in DMEM/F12 (#11320033) based growth medium containing 10% heat -inactivated fetal bovine serum (FBS) (#10500064) and 1x Penicillin-Streptomycin solution (#15140122) until processed in the laboratory (All reagents Thermo Fisher Scientific, Waltham, MA, USA). Primary OM cell cultures were established according to the published protocol [39] with small modifications. In short, any remaining of blood or cartilage were removed under a dissection microscope and the flattened tissue piece was rinsed several times with cold Hank's Balanced Salt Solution. To separate olfactory epithelium and underlying lamina propria, the tissue was enzymatically digested for 45 minutes with dispase II as 2.4 U/ml (Roche, Basel, Switzerland) followed by further digesting the lamina propria with DMEM/F12 media containing 0.25 mg/ml collagenase H (Sigma-Aldrich, St. Louis, MO, USA) for up to 10 minutes. Finally, the digested olfactory epithelium and lamina propria were combined and seeded on poly-D-lysine (Sigma-Aldrich) coated 6-well in order to let the cells migrate out of the tissue pieces and proliferate in growth medium at 37°C, 5% CO_2. One to two days after plating the floating tissue pieces were transferred to new poly-D-lysine coated plates. Half of the culture media was changed every 2-3 days for in total of 8 to 19 days before passaging the cultures and freezing the primary cell lines in liquid nitrogen for later use in solution containing 90 % heat inactivated FBS and 10 % dimethyl sulfoxide. Cells in primary passages of 2-3 were used for scRNA-seq and primary passages 4-6 for biochemical analyses.

APOE-genotyping

APOE-genotyping of the study subjects was performed as described previously [40,41]. Briefly, the genomic DNA was isolated from venous blood samples with QIAamp DNA blood mini extraction kit (QIAGEN) and the *APOE* alleles were determined by polymerase chain reaction for two single-nucleotide polymorphisms (rs429358 and rs7412) with Taqman SNP Genotyping Assays (Applied Biosystems, Foster City, CA, USA). The polymerase chain reaction and following allelic discrimination were performed on QuantStudio 5 Real-Time PCR System platform (Applied Biosystems).

Enzyme-linked immunosorbent assays

The culture medium was collected and cells were lysed in RIPA buffer supplemented with 1x cOMPLETE protease inhibitor cocktail (Roche, Basel, Switzerland). Cell lysates and medium for phosphorylated tau and total tau Enzyme-linked immunosorbent assays (ELISA) were collected in RIPA buffer supplemented with 1x cOmplete protease inhibitor cocktail as well as phosphatase inhibitor cocktail 2 at 1:100 dilution (#P5726, Sigma-Aldrich, MO, USA). Samples were stored at -70°C until analysis. 50 µl of each medium, cell lysate or plasma sample was analyzed in singlets for cell lysates and media samples, and in duplicates for plasma samples using ELISA kits (all from Invitrogen, CA, USA) for human Amyloid beta 40 (#KHB3481), Amyloid beta 42 (#KHB3544), tau (phospho, pT181) (#KHO0631) and tau (total) (#KHB0041), according to the manufacturer's instructions. Total protein amounts of the OM cell lysates were quantified with BCA assay (Pierce™ BCA Protein Assay Kit, Thermo Scientific) according to the manufacturer's instructions. The results were calculated as pg/mg protein ± SD for the OM cells and for plasma samples as pg/ml plasma ± SD.

Cytometric Bead Array for Cytokine Secretion

The cell culture medium was collected and cells were lysed in RIPA buffer supplemented with 1x cOmplete protease inhibitor cocktail (Roche, Basel, Switzerland). 20 µl of each sample was analysed in duplicates using the BD™ CBA Human Soluble Protein Master Kit (#556264; BD Biosciences, CA, USA) alongside the BD™ CBA Human Flex Sets for interleukin 1ß (IL-1ß; #558279), interleukin 6 (IL-6; #558276), interleukin 8 (IL-8; #558277), monocyte chemoattractant protein 1 (MCP-1; #558287), tumour necrosis factor (TNF, #560112). Data were acquired using CytoFLEX S (Beckman Coulter Life Sciences, IN, USA) and analysed with FCAP Array™ v2.0.2 software (Soft flow Inc, MN, USA). Protein concentrations were quantified with BCA kit from the cell lysates as described for the ELISA assays and results were calculated as pg/µg total protein ± SD.

Cell hashing and single cell RNA sequencing

Cells from three cognitively healthy control lines (average age 71.7 years) and two AD patients (average age 72 years), all females with *APOE33* genotype, were harvested from culture with TrypLE Express (Gibco, CA, USA) and resuspended in PBS containing 2% BSA. TotalSeq™ -A anti-human Hashtag Antibodies (BioLegend, San Diego, CA, USA) were used according to the producer's instructions to stain the cells of individual donors before pooling the cells as one pool for control subjects and one pool for AD patients. Equal numbers of cells from each donor were pooled together. Next, the cell pools were filtered through a 30 µm strainer and the cells were resuspended in PBS containing 0.04% BSA. Viability of the single-cell suspension pools was > 90% based on Trypan blue staining.

The sample pools were run on individual lanes of a Chromium Chip B with the Chromium Single Cell 3′ Library & Gel Bead Kit v3 kit (10x Genomics, CA, USA) according to the manufacturer's

protocol with a targeted cell recovery of 10,000 cells per lane. In the cDNA amplification step, the cell hashing protocol from New York Genome Center Technology Innovation Lab (version 2019-02-13) was followed (https://genomebiology.biomedcentral.com/articles/10.1186/s13059-018-1603-1). The hashtag oligonucleotide primer (HTO primer 5'GTGACTGGAGTTCAGACGTGTGCTC'3) was added to the cDNA amplification mix. During cDNA cleanup, the supernatant contained the HTO-derived cDNAs (<180bp) and the pellet the mRNA-derived cDNAs (>300bp). The mRNA-derived cDNAs were processed according to the protocol provided by 10x Genomics and the HTO-derived cDNAs fraction was processed according to the cell hashing protocol referenced above. The 3' gene expression libraries and HTO sequencing libraries were pooled and sequenced at an approximate depth of 50,000 reads per cell for the 3' gene expression libraries and 5,000 reads for HTO libraries using the NovaSeq S1 (Illumina, San Diego, CA, USA) flow cells.

Single cell RNA sequencing analysis

Cell Ranger v.3.0.2 was used to analyze the raw base call files. FASTQ files and raw gene-barcode matrices were generated using the command 'mkfastq' and the 'count' respectively and aligned human genome GRCh37 (hg19). Thereafter, we integrate the samples in R v.3.5.2 and the two integrated Seurat objects, one of AD samples and one of control samples, were analyzed using the Seurat package v.3.1 [40,41]. Using the standard integration workflow (https://satijalab.org/seurat/v3.0/integration.html) we separately combined the control and AD samples dataMatrix, samples were normalized with the NormalizeData() function using the centered log-ratio (CLR) transformation and then, with the two samples separated, we ran Seurat's HTODemux with default parameters on the hashtag-count matrix to demultiplex interested cell

barcodes. We checked the HTO count distribution, classified cells into singlet/doublet/negative and then we removed doublets using the subset() function. To assign single cells back to their sample origins we used the Seurat function HTODemux() with the following parameter data.SeuratObj.Control <- HTODemux(data.SeuratObj.Control, assay="HTO", positive.quantile = 0.99, kfunc = "kmeans", verbose=T). After demultiplexing step, analyzing the QC parameters, we performed the cells filtering separately for the two libraries removing low-quality cells with nFeature> 750 and nFeature_RNA < 7000, nCount_RNA < 40000, and mitochondrial content < 12%. The function SplitObject() was used to separate each donor inside the AD and controls samples. Each of them was then normalized using the NormalizeData() function and the most 5000 variable features were extracted using the FindVariableFeatures() function applying the vst() method. Thereafter, for each separate library, we proceeded with the integration of the samples. At first we extracted the anchors between samples using the 5000 features before with the FindIntegrationAnchors() function and the first 30 dimensions, then, with the extracted anchors we integrated the samples cells also using the first 30 dimensions and the IntegrateData() function. Each of the objects in these two libraries were then scaled and the PCA was applied using the RunPCA() function. We used the first 30 dimensions for each dataset and then computed the clustering for each of them using the FindClusters() function. Two different clustering resolutions were used for the two datasets: 0.4 for the AD and 1.4 for the control. The RunUMAP() function was used to apply the UMAP dimensional reduction.

For each cluster the top 30 over-expressed genes were identified with FindAllMarkers() function using the Wilcox rank sum test and setting the min.pct and logfc.threshold parameters to 0.3. The top significant genes were inputted, for the cell-type annotation, into EnrichR and HumanBase tools, using Gene Ontology and cellular pathway to verify the output results. Clusters 1 and 12 in

control library were analyzed separately from the others to obtain a more confident annotation, the cells were clustered with a resolution of 0.2 and then the two sub-clusters obtained were merged with the other clusters after the cell-type annotation.

To have a complete overview of the data, the AD and control samples were integrated together with the SCTransform pipeline provided by Seurat. 5000 features were selected to integrate the samples using the SelectIntegrationFeatures() function, all the necessary residuals were calculated with the PrepSCTIntegration() function and the anchors for the integration were extracted using the first 30 dimensions. Data were integrated with the IntegrateData() function and PCA was performed to obtain the dimensionality reduction. Cells were clustered with the standard resolution of 0.8 and the RunUMAP() function was used to carry out a two dimensional spatial visualization of the cells.

Differential gene expression and pathway enrichment analysis

The differential gene expression was performed using the function FindMarkers() between AD and control libraries, and between subpopulations of cells in common between AD and controls. To perform the pathway enrichment analysis and to understand in which biological processes the differential expressed genes are involved a non-parametric unsupervised method called Gene Set Variation Analysis (GSVA, v1.38.0) was used.

Statistical methods and graphical illustrations

GraphPad Prism 8.1.0 (GraphPad Software Inc. San Diego, CA, USA) software was used for statistical analysis of the data. Mean values in ELISA and CBA analyses, between control and AD, was compared using unpaired t-test with Welch's correction or with two-way ANOVA. Error bars

in the figure legends represent standard deviation (SD). Statistical significance was assumed for *p*-values < 0.05. The graphical illustrations were created with BioRender.com and open source vector graphics editor Inkscape 0.91.

Acknowledgements

The authors would like to thank Ratneswary Sutharsan for assistance in establishing the OM culture conditions and Mirka Tikkanen for technical assistance. We gratefully acknowledge the support of The Academy of Finland, The Juselius Foundation, The Finnish Cultural Foundation, The Inkeri and Mauri Vänskä Foundation, The Yrjö Jahnsson Foundation, The Saastamoinen Foundation and The Finnish Brain Foundation. Sequencing was performed by the Sequencing unit of Institute for Molecular Medicine Finland FIMM Technology Centre, University of Helsinki. Sequencing unit it supported by Biocenter Finland.

REFERENCES

1. Marin, C. *et al.* Olfactory Dysfunction in Neurodegenerative Diseases. *Current Allergy and Asthma Reports* **18**, 42 (2018).
2. Jung, H. J., Shin, I.-S. & Lee, J.-E. Olfactory function in mild cognitive impairment and Alzheimer's disease: A meta-analysis. *The Laryngoscope* **129**, 362–369 (2019).
3. Lane, C. A., Hardy, J. & Schott, J. M. Alzheimer's disease. *European Journal of Neurology* vol. 25 59–70 (2018).
4. Kim, Y. H. *et al.* Amyloid beta in nasal secretions may be a potential biomarker of Alzheimer's disease. *Scientific Reports* **9**, 4966 (2019).
5. Liu, Z. *et al.* Development of a High-Sensitivity Method for the Measurement of Human Nasal Aβ 42, Tau, and Phosphorylated Tau. *Journal of Alzheimer's Disease* **62**, 737–744 (2018).
6. Yoo, S. J. *et al.* Longitudinal profiling of oligomeric Aβ in human nasal discharge reflecting cognitive decline in probable Alzheimer's disease. *Scientific Reports* **10**, 11234 (2020).

7. Ayala-Grosso, C. A. *et al.* Amyloid-Aβ peptide in olfactory mucosa and mesenchymal stromal cells of mild cognitive impairment and Alzheimer's disease patients. *Brain Pathology* **25**, 136–145 (2015).

8. Arnold, S. E. *et al.* Olfactory epithelium amyloid-β and paired helical filament-tau pathology in Alzheimer disease. *Annals of Neurology* **67**, 462–469 (2010).

9. Talamo, B. R. *et al.* Pathological changes in olfactory neurons in patients with Alzheimer's disease. *Nature* **337**, 736–739 (1989).

10. Lee, J. H., Goedert, M., Hill, W. D., Lee, V. M. Y. & Trojanowski, J. Q. Tau Proteins Are Abnormally Expressed in Olfactory Epithelium of Alzheimer Patients and Developmentally Regulated in Human Fetal Spinal Cord. *Experimental Neurology* **121**, 93–105 (1993).

11. Ghanbari, H. A. *et al.* Oxidative damage in cultured human olfactory neurons from Alzheimer's disease patients. *Aging Cell* vol. 3 41–44 (2004).

12. Wolozin, B., Lesch, P., Lebovics, R. & Sunderland, T. Olfactory neuroblasts from Alzheimer donors: Studies on APP processing and cell regulation. *Biological Psychiatry* **34**, 824–838 (1993).

13. Durante, M. A. *et al.* Single-cell analysis of olfactory neurogenesis and differentiation in adult humans. *Nature Neuroscience* **23**, 323–326 (2020).

14. Holbrook, E. H., Rebeiz, L. & Schwob, J. E. Office-based olfactory mucosa biopsies. *International Forum of Allergy and Rhinology* **6**, 646–653 (2016).

15. Mi, H., Muruganujan, A., Ebert, D., Huang, X. & Thomas, P. D. PANTHER version 14: More genomes, a new PANTHER GO-slim and improvements in enrichment analysis tools. *Nucleic Acids Research* **47**, D419–D426 (2019).

16. Mi, H. & Thomas, P. PANTHER pathway: an ontology-based pathway database coupled with data analysis tools. *Methods in molecular biology (Clifton, N.J.)* **563**, 123–140 (2009).

17. Liu, Z. *et al.* Development of a High-Sensitivity Method for the Measurement of Human Nasal Aβ 42, Tau, and Phosphorylated Tau. *Journal of Alzheimer's Disease* **62**, 737–744 (2018).

18. Kameshima, N., Nanjou, T., Fukuhara, T., Yanagisawa, D. & Tooyama, I. Correlation of Aβ deposition in the nasal cavity with the formation of senile plaques in the brain of a transgenic mouse model of Alzheimer's disease. *Neuroscience Letters* **513**, 166–169 (2012).

19. Lopez-Perez, E., Seidah, N. G. & Checler, F. Proprotein Convertase Activity Contributes to the Processing of the Alzheimer's β-Amyloid Precursor Protein in Human Cells: Evidence for a Role of the Prohormone Convertase PC7 in the Constitutive -Secretase Pathway. *Journal of Neurochemistry* **73**, 2056–2072 (2002).

20. Py, N. A. *et al.* Differential spatio-temporal regulation of MMPs in the 5xFAD mouse model of Alzheimerâ€™s disease: evidence for a pro-amyloidogenic role of MT1-MMP. *Frontiers in Aging Neuroscience* **6**, 247 (2014).

21. Park, B. H., Kim, H. G., Jin, S. W., Song, S. G. & Jeong, H. G. Metallothionein-III increases ADAM10 activity in association with furin, PC7, and PKCα during non-amyloidogenic processing. *FEBS Letters* **588**, 2294–2300 (2014).

22. Lanni, C. *et al.* Homeodomain Interacting Protein Kinase 2: A Target for Alzheimer's Beta Amyloid Leading to Misfolded p53 and Inappropriate Cell Survival. *PLoS ONE* **5**, e10171 (2010).

23. Esteve, P. *et al.* Elevated levels of Secreted-Frizzled-Related-Protein 1 contribute to Alzheimer's disease pathogenesis. *Nature Neuroscience* **22**, 1258–1268 (2019).

24. Kovacs, G. G. Astroglia and Tau: New Perspectives. *Frontiers in Aging Neuroscience* vol. 12 (2020).

25. Lambert, J. C. *et al.* Implication of the immune system in Alzheimer's disease: evidence from genome-wide pathway analysis. *Journal of Alzheimer's Disease* **20**, 1107–1118 (2010).

26. Jones, L. *et al.* Correction: Genetic Evidence Implicates the Immune System and Cholesterol Metabolism in the Aetiology of Alzheimer's Disease. *PLoS ONE* **6**, (2011).

27. Jiang, Q. *et al.* Alzheimer's Disease Variants with the Genome-Wide Significance are Significantly Enriched in Immune Pathways and Active in Immune Cells. *Molecular Neurobiology* **54**, 594–600 (2017).

28. Pillai, J. A. *et al.* Key inflammatory pathway activations in the MCI stage of Alzheimer's disease. *Annals of Clinical and Translational Neurology* **6**, 1248–1262 (2019).

29. Chen, J. *et al.* Gene expression analysis reveals the dysregulation of immune and metabolic pathways in Alzheimer's disease. *Oncotarget* **7**, (2016).

30. Kandimalla, R. & Reddy, P. H. Therapeutics of Neurotransmitters in Alzheimer's Disease. *Journal of Alzheimer's Disease* vol. 57 1049–1069 (2017).

31. Chew, S. *et al.* Urban air particulate matter induces mitochondrial dysfunction in human olfactory mucosal cells. *Particle and Fibre Toxicology* **17**, 18 (2020).

32. Murphy, C. Olfactory and other sensory impairments in Alzheimer disease. *Nature Reviews Neurology* vol. 15 11–24 (2019).

33. Grubman, A. *et al.* A single-cell atlas of entorhinal cortex from individuals with Alzheimer's disease reveals cell-type-specific gene expression regulation. *Nature Neuroscience* **22**, 2087–2097 (2019).

34. Vitale, A. M. *et al.* DNA methylation in schizophrenia in different patient-derived cell types. *npj Schizophrenia* **3**, 6 (2017).

35. Penney, J., Ralvenius, W. T. & Tsai, L. H. Modeling Alzheimer's disease with iPSC-derived brain cells. *Molecular Psychiatry* vol. 25 148–167 (2020).

36. Jack, C. R. *et al.* NIA-AA Research Framework: Toward a biological definition of Alzheimer's disease. *Alzheimer's and Dementia* vol. 14 535–562 (2018).

37. Morris, J. C. *et al.* The consortium to establish a registry for alzheimer's disease (CERAD). Part I. Clinical and neuropsychological assessment of alzheimer's disease. *Neurology* **39**, 1159–1165 (1989).

38. Mirra, S. S. *et al.* The consortium to establish a registry for Alzheimer's disease (CERAD). Part II. Standardization of the neuropathologic assessment of Alzheimer's disease. *Neurology* **41**, 479–486 (1991).

39. Murrell, W. *et al.* Multipotent stem cells from adult olfactory mucosa. in *Developmental Dynamics* vol. 233 496–515 (John Wiley & Sons, Ltd, 2005).

40. Stuart, T. *et al.* Comprehensive Integration of Single-Cell Data. *Cell* **177**, 1888-1902.e21 (2019).

41. Butler, A., Hoffman, P., Smibert, P., Papalexi, E. & Satija, R. Integrating single-cell transcriptomic data across different conditions, technologies, and species. *Nature Biotechnology* **36**, 411–420 (2018).